

## 7.4 Metal-organic frameworks

Christoph Janiak

Metal-organic frameworks, abbreviated as MOFs, are coordination networks with organic ligands containing potential voids. Coordination networks are cross-linked metal coordination compounds extending through repeating coordination entities in two or three dimensions (2D, 3D) [1]. Porosity is usually determined after removal of the templating solvent molecules by measuring a nitrogen (or argon) sorption isotherm at 77 K (78 K) and then calculating an internal surface area and pore size distribution based on the Brunauer-Emmett-Teller (BET) theory and related to 1.0 g material (specific surface area). The four prototypical MOFs MOF-5, Cu-btc, MIL-53 (Al) and ZIF-8 will be briefly presented.

### 7.4.1 Selected MOF structures

MOF-5: Based on hydrothermally obtained tetranuclear and tetrahedral  $\{Zn_4(\mu_4-O)\}$  units and aromatic para-dicarboxylate ligands such as benzene-1,4-dicarboxylate ( $bdc^{2-}$ , terephthalate), a series of similarly constructed (iso-reticular) structures, including 3D- $[Zn_4O(bdc)_3]$ , MOF-5, can be obtained [2]. The carboxylate groups span the six edges of the  $\{Zn_4(\mu_4-O)\}$  tetrahedron, and the dicarboxylate bridges are oriented at right angles to each other (Figure 7.4.1).

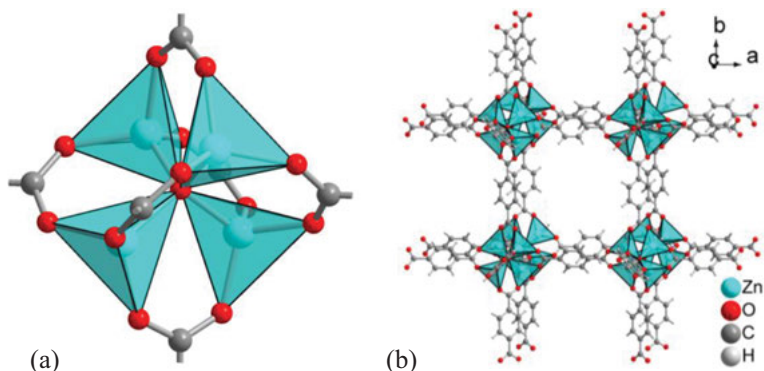


**Figure 7.4.1:** (a) Tetranuclear  $\{Zn_4(\mu_4-O)\}$  unit of MOF-5 with bridging carboxylate groups. The C atoms of the carboxylate bridge are located at the vertices of an octahedron. Each Zn atom is tetrahedrally coordinated by four O atoms. (b) Packing diagram of 3D- $[Zn_4O(bdc)_3]$ , MOF-5. The network is traversed by channels along the *a*, *b* and *c* axis. The specific internal surface area is  $\sim 2900 \text{ m}^2 \text{ g}^{-1}$ .

**Cu-btc:** The compound  $3\text{D}[\text{Cu}_3(\text{btc})_2(\text{H}_2\text{O})_3]$  (also called HKUST-1,  $\text{btc}^{3-}$  = benzene-1,3,5-tricarboxylate, trimesate) contains two copper atoms as the metal atom assembly, which are bridged by four carboxylate groups as in copper acetate ( $[\text{Cu}_2(\text{CH}_3\text{COO})_4]$ ) to form a “paddle-wheel” unit (Figure 7.4.2). Cu-btc is stable up to 240 °C. The aqua ligands can be removed [3].

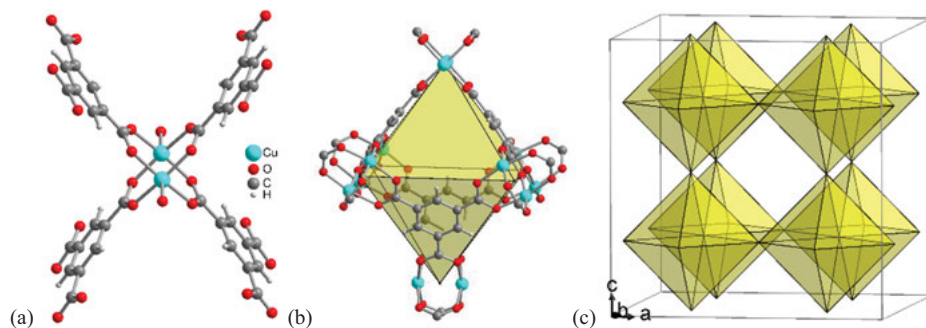


**Figure 7.4.2:** (a)  $\{\text{Cu}_2(\text{btc})_4\}$  “paddle-wheel” unit in Cu-btc (HKUST-1). (b) The  $\{\text{Cu}_2\}$  dumbbells sit at the corners of an octahedron. Four btc ligands each span opposite four of the eight faces of the octahedron. (c) These octahedra form a porous 3D network via vertex linkage. The network is traversed by channels along the  $a$ ,  $b$  and  $c$  axis. The specific surface area is  $\sim 1300 \text{ m}^2 \text{ g}^{-1}$ .

**MIL-53(Al):** Many aluminum MOFs with the formula unit  $3\text{D}[\text{Al}(\mu\text{-OH})(\text{dicarboxylate ligand})]$  such as MIL-53(Al), are built up from slightly angled strands of vertex-sharing  $\{\text{AlO}_6\}$  octahedra. In the strands, the Al atoms are connected by the oxygen atoms of  $\mu$ -hydroxido and carboxylate bridges (Figure 7.4.3) [4]. The dicarboxylate ligands connect each strand to four neighboring strands, forming microporous rhombic to square channels in the 3D framework. The dicarboxylate ligands are terephthalate in MIL-53(Al).

**ZIF-8:** Three-dimensional zeolitic imidazolate frameworks (ZIFs) with the formula  $3\text{D}[\text{Zn}(\text{imidazolate})_2]$  are obtained from  $\text{Zn}^{2+}$  and imidazolate ligands. ZIFs are one of the few porous MOFs in which individual metal atoms are bridged by ligands. In ZIFs, each Zn atom is surrounded by four N atoms from four imidazolate ligands (Figure 7.4.4). The linkage leads to zeolite-like structures in which the Zn atom occupies the position of Al/Si and the imidazolate bridges occupy the positions of the oxygen bridges in the zeolite. The best-known ZIF is ZIF-8 with 2-methylimidazolate as ligand [5, 6].

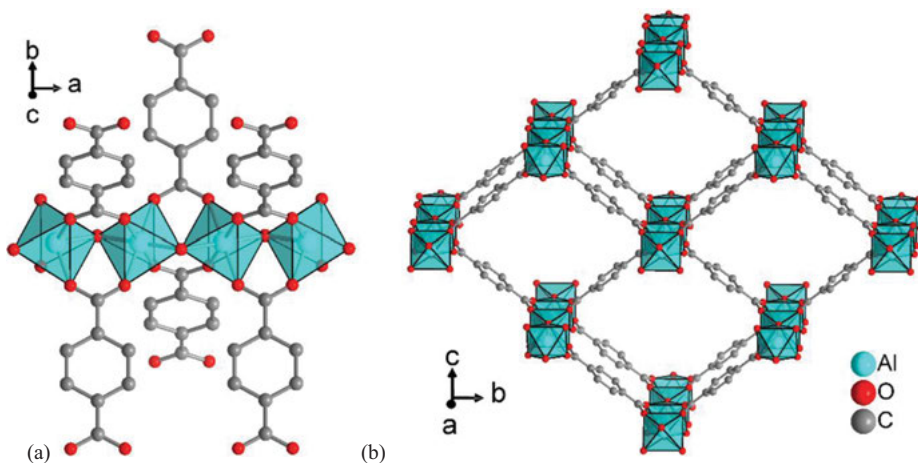


**Figure 7.4.3:** (a) Vertex-linked  $\{\text{Al}(\mu\text{-OH})(\text{O}_2\text{C-C}_6\text{H}_4\text{-CO}_2)_2\}$  strand in MIL-53(Al) and (b) resulting 3D framework with parallel channels in only one direction (here along a) (hydrogen atoms are not shown). The specific surface area is  $1600 \text{ m}^2 \text{ g}^{-1}$  for (the large-pore form of) MIL-53(Al).

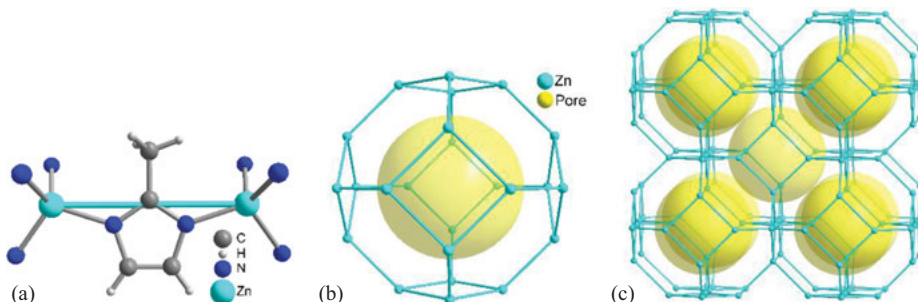


**Figure 7.4.4:** (a) Zn and 2-methylimidazolate building groups in ZIF-8 and (b) the assembly to a  $\beta$ -cage and (c) sodalite structure showing only the Zn atoms and their topological connections. The pore represented by the yellow sphere inside the  $\beta$ -cage has a diameter of  $12 \text{ \AA}$ ; the hexagonal rings as pore openings have a diameter of  $3.4 \text{ \AA}$  (taking the van-der-Waals surface into account). The BET surface area is about  $1600 \text{ m}^2 \text{ g}^{-1}$ .

### 7.4.2 General MOF properties

MOFs are crystalline microporous to mesoporous materials (microporous  $< 2 \text{ nm}$ , mesoporous from  $2$  to  $50 \text{ nm}$  pore diameter). In contrast to the amorphous mesoporous materials silica gel and activated carbons, MOFs have defined identical pore systems due to their crystallinity. In contrast to the likewise crystalline and thus uniform microporous zeolites with only limited structural units, the pore size and shape, the hydrophilicity/hydrophobicity, the inner surface functionality up to the chirality can be tailored in many ways in MOFs by the organic bridging ligands. The

ligands can be modified by organic-chemical reactions (substitutions, additions) even after the formation of the MOF network. For this purpose, the term “post-synthetic modification” has been coined for MOFs [7].

There are now about 200 zeolite structures compared to over 20000 MOF structures. The BET surface area for zeolites, silica gels and activated carbons is at most about  $1000 \text{ m}^2 \text{ g}^{-1}$ , while values of  $2000\text{--}4000 \text{ m}^2 \text{ g}^{-1}$  are reproducible and applicable for MOFs. The pore openings or channel diameters in MOFs range from 0.3 to 3.4 nm, with specific pore volumes up to  $1.5\text{--}2 \text{ cm}^3 \text{ g}^{-1}$ .

From the synthesis, the pores of the MOF scaffolds are filled with solvent molecules, which have a templating effect. Before using the porosity, the solvent guest molecules have to be removed, which is done by evacuation, if necessary after an exchange of less volatile for more volatile solvents. In this way, the MOF is first activated.

Some MOFs are already being produced industrially on a pilot scale in anticipation of applications. Without going into details of MOF synthesis, there is the problem of “greener”, cheaper and easily scalable synthesis procedures to provide access to larger amounts if these materials are to be used. The synthetic procedures for fabricating MOFs can require harsh conditions (high temperature/high pressure in autoclaves) and/or expensive organic linkers together with not environmentally benign solvents. There is the need to develop more syntheses at ambient pressures, possibly as continuous processes and without the often-used organic solvents like dimethylformamide [8, 9]. A positive example is the MOF aluminum fumarate ( $[\text{Al}(\text{OH})(\text{O}_2\text{C}-\text{C}_2\text{H}_2-\text{CO}_2)]$ , BASOLITE<sup>TM</sup> A520) [10, 11], where only aqueous solutions of aluminum sulfate and sodium fumarate are combined at ambient pressure and at a temperature of  $60 \text{ }^\circ\text{C}$ , even in a continuous flow process with a space-time-yield of  $97159 \text{ kg m}^{-3} \text{ day}^{-1}$  and a rate of  $5.6 \text{ kg h}^{-1}$  [12].

From the initial synthesis, MOFs are prepared as microcrystalline powders. Yet, powdered MOFs have limited practical interest owing to poor processability, safety problems from dusting and poor recyclability. The use of MOFs in potential applications most often requires shaping as an important aspect of their prospective use at an industrial scale. Thus, MOFs have to be formulated to obtain handable objects as deposited MOF layers on a substrate, coatings, films or 3D-structured composites such as grains, pellets, beads, areogels, hydrogels and monoliths (Figure 7.4.5) [13–15]. These shaped MOF particles have to be mechanically stable and retain the initial MOF porosity [16]. The simple use of a polymeric binder to assemble and shape MOF particles to a larger object may block the MOF pores and reduce the accessible surface area.

A possible obstacle for applications of MOFs is their often-insufficient hydrothermal stability [17] even if by now, some MOFs are known to be stable against prolonged contact with water and humid air.

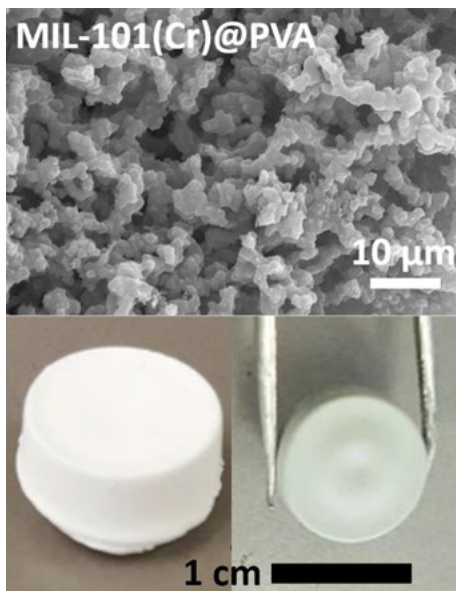


**Figure 7.4.5:** MOF@polymer-monolith composites (with a scanning electron microscopy image) from the MOFs Al-fumarate (left) and MIL-101(Cr) (right) with the polymer poly(vinyl alcohol) (PVA), prepared using a phase separation technique. In the MOF@PVA monoliths, the mass-weighted BET surface area and the water vapor uptake capacity reproducibly reached 60–100% of the neat MOF values with MOF loadings of 50–80 wt%. The monoliths exhibit slightly plastic properties and a high resistance against deformation.

### 7.4.3 Potential applications of MOFs

In terms of industrial scale applications, MOFs can still be seen as an emerging class of materials. So far, most of the noted “applications” have to be regarded as potential ones and have to do with the porosity. MOFs are intensively investigated for a task- and compound-specific selective adsorption, storage and separation, sensing, catalysis, etc. For many of the applications, it is mandatory to develop robust and inexpensive MOF materials with good hydrolytic stability, excellent adsorption properties and recyclability.

The following paragraphs summarize the most important “application-oriented” developments with MOFs [18], based on review articles, but they do not present a full account of all “possible applications”. It should also be noted that there are occasional applications with “MOFs” which have no proven porosity and are rather non-porous coordination polymer/network. The noted possible applications do not only refer to pristine MOFs but also refer to MOF composites, for example, mixed-matrix membranes for gas separation with MOFs as fillers [19, 20].

Early on, MOFs came into the focus for H<sub>2</sub> storage for mobile applications. At 77 K, volume-specific storage curves of hydrogen on different MOF-materials in comparison to the compression curve of hydrogen into empty gas containers showed an up to three times higher H<sub>2</sub> uptake in g(H<sub>2</sub>)/L(container). Still, a sufficiently high amount of storage at room temperature could not be attained [21, 22]. For methane, the storage capacity of a tank filled with shaped bodies of the MOF Basolite A520 could reach a 40% increase vs. a conventional container at 35 bar and room temperature [10].

Numerous studies have demonstrated the capture and separation of carbon dioxide, CO<sub>2</sub> from binary mixtures with N<sub>2</sub>, which were simplistically viewed as flue gas [23, 24] as well as of SO<sub>2</sub>, H<sub>2</sub>S, NH<sub>3</sub> and NO<sub>x</sub> from gas mixtures [25, 26] and even up to chemical warfare agents [27]. MOFs have addressed the adsorption-based separations of fluorocompounds [28], acetylene/ethylene [29], olefin/paraffin, linear/branched alkanes, xenon/krypton [30], acetylene/CO<sub>2</sub> [31], hydrogen isotopes [32] and adsorption-based purifications, of e.g. ethylene [33].

MOFs have been investigated for the ionic conduction of various charge carriers, such as a proton ( $>10^{-2}$  S cm<sup>-1</sup>), hydroxide ion ( $>10^{-2}$  S cm<sup>-1</sup>), lithium ion, sodium ion and magnesium ion (all about 10<sup>-4</sup> S cm<sup>-1</sup>) in their pores [34, 35] as well as for energy applications such as electrocatalysts [36], energy storage and conversion [37], supercapacitors [38], batteries and fuel cells [39].

MOFs have been developed for their possible use as sensors for the detection of many different gases and volatile organic compounds [40, 41], as signal amplification elements for electrochemical sensing [42], for the sensing and imaging of biomolecules [43, 44], environmental pollutants [45], explosives [46], ionic species [47, 48], among many others. Often, the luminescence of MOFs from the linkers, metals, incorporated luminophores or a combination thereof is utilized for the sensing application [49–51].

MOFs are used as size- and enantioselective heterogeneous catalysts [52, 53], including enzyme-MOF composites with MOFs as an enzyme immobilization platform [54, 55], as solid catalysts for liquid-phase continuous flow reactions [56], for the photocatalytic degradation of dyes in water depollution [57], etc.

MOFs are studied for the adsorptive removal of synthetic dyes in textile effluents [58] as well as of pharmaceuticals, personal care products [59] and of fluoride and arsenic [60] from (waste)water.





The porosity of MOFs enables them to be used for (self-sacrificial) drug delivery [61–63], including the sustained release of antibiotic and antimicrobial drugs [64] or bisphosphonate anti-osteoporotic drugs [65].

MOFs are investigated as materials for adsorption and desiccant cooling technologies through cyclic sorption of water or methanol in adsorption-driven heat pumps or adsorption chillers [66–70]. The aspect of cyclic water sorption extends to water harvesting from air for fresh water production [71–73].

In 2016, the first commercial application of a MOF may have materialized. The MOF (by the company MOF Technologies) was used to store and release 1-methylcyclopropene (1-MCP) to slow the fruit ripening process. 1-MCP binds and blocks ethylene receptors in the fruit, with ethylene being a ripening hormone [74, 75].


The MOF start-up NuMat is supplying MOF-filled gas storage cylinders, named ION-X, to store toxic gases (e.g. arsine, phosphine and boron trifluoride), which are used as dopants in the semiconductor industry, and doing this more safely than conventional pressurized cylinders [73, 76].

## References

-  [1] Batten SR, Champness NR, Chen XM, Garcia-Martinez J, Kitagawa S, Öhrström L, O’Keeffe M, Paik Suh M, Reedijk J. *Pure Appl Chem*, 2013, 85, 1715–24.
- [2] Eddaoudi M, Kim J, Rosi N, Vodak D, Wachter J, O’Keeffe M, Yaghi OM. *Science*, 2002, 295, 469–72.
- [3] Chui SSY, Lo SMF, Charmant JPH, Orpen AG, Williams ID. *Science*, 1999, 283, 1148–50.
- [4] Serre C, Millange F, Thouvenot C, Nogues M, Marsolier G, Louer D, Férey G. *J Am Chem Soc*, 2002, 124, 13519–26.
- [5] Huang XC, Lin YY, Zhang JP, Chen XM. *Angew Chem Int Ed*, 2006, 45, 1557–59.
- [6] Park KS, Ni Z, Cote AP, Choi JY, Huang R, Uribe-Romo FJ, Chae HK, O’Keeffe M, Yaghi OM. *Proc Natl Acad Sci USA*, 2006, 103, 10186–91.
- [7] Cohen S. *Chem Rev*, 2012, 112, 970–1000.
- [8] El-Sayed EM, Yuan D. *Green Chem*, 2020, 22, 4082–104.
- [9] Reinsch H, Stock N. *Dalton Trans*, 2017, 46, 8339–49.
-  [10] (a) Yilmaz B, Trukhan N, Müller U. *Chin J Catal*, 2012, 33, 3–10. [https://doi.org/10.1016/S1872-2067\(10\)60302-6](https://doi.org/10.1016/S1872-2067(10)60302-6). (b) Gaab M, Trukhan N, Maurer S, Gummaraju R, Müller U. *Microporous Mesoporous Mater*, 2012, 157, 131–6.
- [11] Jeremias F, Fröhlich D, Janiak C, Henninger SK. *RSC Adv*, 2014, 4, 24073–82.
- [12] Rubio-Martinez M, Hadley TD, Batten MP, Constanti-Carey K, Barton T, Marley D, Mçnch A, Lim KS, Hill MR. *Chem Sus Chem*, 2016, 9, 938–41.
- [13] Wang LY, Xu H, Gao JK, Yao JM, Zhang QC. *Coord Chem Rev*, 2019, 398, 213016.
- [14] Cheng P, Wang C, Kaneti YV, Eguchi M, Lin J, Yamauchi Y, Na J. *Langmuir*, 2020, 36, 4231–49.
- [15] Meng J, Liu X, Niu C, Pang Q, Li J, Liu F, Liuu Z, Mai L. *Chem Soc Rev*, 2020, 49, 3142–86.
- [16] Bazer-Bachi D, Assié L, Lecoq V, Harbuzaru B, Falk V. *Powder Technol*, 2014, 255, 52–59.
- [17] Leus K, Bogaerts T, De Decker J, Depauw H, Hendrickx K, Vrielinck H, Van Speybroeck V, Van Der Voort P. *Microporous Mesoporous Mater*, 2016, 226, 110–16.
-  [18] Silva P, Vilela SMF, Tomé JCP, Paz FAA. *Chem Soc Rev*, 2015, 44, 6774–803.
- [19] Dechnik J, Sumbly CJ, Janiak C. *Cryst Growth Des*, 2017, 17, 4467–88.
- [20] Dechnik J, Gascon J, Doonan CJ, Janiak C, Sumbly CJ. *Angew Chem Int Ed*, 2017, 56, 9292–310.
-  [21] Mueller U, Schubert M, Teich F, Puetter H, Schierle-Arndt K, Pastré J. *J Mater Chem*, 2006, 16, 626–36.
- [22] Paik Suh M, Park HJ, Prasad TK, Lim DW. *Chem Rev*, 2012, 112, 782–835.
- [23] Zhang Z, Zhao Y, Gong Q, Li Z, Li J. *Chem Commun*, 2013, 49, 653–61.
- [24] Sumida K, Rogow DL, Mason JA, McDonald TM, Bloch ED, Herm ZR, Bae TH, Long JR. *Chem Rev*, 2012, 112, 724–81.

- [25] Martínez-Ahumada E, López-Olvera A, Jancik V, Sánchez-Bautista JE, González-Zamora E, Martis V, Williams DR, Ibarra IA. *Organometallics*, 2020, 39, 883–915.
- [26] Martínez-Ahumada E, Díaz-Ramírez ML, de Velásquez-Hernández MJ, Jancik V, Ibarra IA. *Chem Sci*, 2021, 12, 6772–99.
- [27] Islamoglu T, Chen Z, Wasson MC, Buru CT, Kirlikovali KO, Afrin U, Rasel Mian M, Farha OK. *Chem Rev*, 2020, 120, 8130–60.
- [28] Wanigarathna DKJA, Gao J, Liu B. *Mater Adv*, 2020, 1, 310–20.
- [29] Hua GF, Xie XJ, Lu W, Li D. *Dalton Trans*, 2020, 49, 15548–59.
- [30] Adil K, Belmabkhout Y, Pillai RS, Cadiau A, Bhatt PM, Assen AH, Maurin G, Eddaoudi M. *Chem Soc Rev*, 2017, 46, 3402–30.
- [31] Fu XP, Wang YL, Liu QY. *Dalton Trans*, 2020, 49, 16598–607.
- [32] Ju Z, El-Sayed ESM, Yuan D. *Dalton Trans*, 2020, 49, 16617–22.
- [33] Liu S, Dong Q, Zhou Y, Wang S, Duan J. *Dalton Trans*, 2020, 49, 17093–105.
- [34] Sadakiyo M, Kitagawa H. *Dalton Trans*, 2021, 50, 5385–97.
- [35] Bhardwaj SK, Bhardwaj N, Kaur R, Mehta J, Sharma AL, Kim KH, Deep A. *J Mater Chem A*, 2018, 6, 14992–5009.
- [36] Li L, He J, Wang Y, Lv X, Gu X, Dai P, Liu D, Zhao X. *J Mater Chem A*, 2019, 7, 1964–88.
- [37] Wang K, Nam Hui K, San Hui K, Peng S, Xu Y. *Chem Sci*, 2021, 12, 5737–66.
- [38] Pei C, Sung Choi M, Yu X, Xue H, Xia BY, Seok Park H. *J Mater Chem A*, 2021, 9, 8832–69.
- [39] Kuyuldar S, Genna DT, Burda C. *J Mater Chem A*, 2019, 7, 21545–76.
- [40] Yao MS, Li WH, Xu G. *Coord Chem Rev*, 2021, 426, 213479.
- [41] Li HY, Zhao SH, Zang SQ, Li J. *Chem Soc Rev*, 2020, 49, 6364–401.
- [42] Liu S, Lai C, Liu X, Li B, Zhang C, Qin L, Huang D, Yi H, Zhang M, Li L, Wang W, Zhou X, Chen L. *Coord Chem Rev*, 2020, 424, 213520.
- [43] Dong J, Zhao D, Lu Y, Sun WY. *J Mater Chem A*, 2019, 7, 22744–67.
- [44] Duman FD, Forgan RS. *J Mater Chem B*, 2021, 9, 3423–49.
- [45] Rosales-Vázquez LD, Dorazco-González A, Sánchez-Mendieta V. *Dalton Trans*, 2021, 50, 4470–85.
- [46] Dutta A, Singh A, Wang X, Kumar A, Liu J. *CrystEngComm*, 2020, 22, 7736–81.
- [47] Kaur H, Sinha S, Krishnan V, Rani Koner R. *Dalton Trans*, 2021, 50, 8273–91.
- [48] Panda SK, Mishra S, Singh AK. *Dalton Trans*, 2021, 50, 7139–55.
- [49] Lustig WP, Mukherjee S, Rudd ND, Desai AV, Li J, Ghosh SK. *Chem Soc Rev*, 2017, 46, 3242–85.
- [50] Hazra A, Mondal U, Mandal S, Banerjee P. *Dalton Trans*, 2021, 50, 8657–70.
- [51] Zhao Y, Li D. *J Mater Chem C*, 2020, 8, 12739–54.
- [52] Qin JS, Yuan S, Lollar C, Pang J, Alsalmé A, Zhou HC. *Chem Commun*, 2018, 54, 4231–49.
- [53] Rogge SMJ, Bavykina A, Hajek J, Garcia H, Olivos-Suarez AI, Sepúlveda-Escribano A, Vimont A, Clet G, Bazin P, Kapteijn F, Daturi M, Ramos-Fernandez EV, Llabrés I Xamena FX, Van Speybroeck V, Gascon J. *Chem Soc Rev*, 2017, 46, 3134–84.
- [54] Lian X, Fang Y, Joseph E, Wang Q, Li J, Banerjee S, Lollar C, Wang X, Zhou HC. *Chem Soc Rev*, 2017, 46, 3386–401.
- [55] Majewski MB, Howarth AJ, Li P, Wasielewski MR, Hupp JT, Farha OK. *CrystEngComm*, 2017, 19, 4082–91.
- [56] Dhakshinamoorthy A, Navalon S, Asiri AM, Garcia H. *Chem Commun*, 2020, 56, 26–45.
- [57] Sharma VK, Feng M. *J Hazard Mater*, 2019, 372, 3–16.
- [58] Parmar B, Bisht KK, Rajput G, Suresh D. *Dalton Trans*, 2021, 50, 3083–108.
- [59] Jin E, Lee S, Kang E, Kim Y, Choe W. *Coord Chem Rev*, 2020, 425, 213526.
- [60] Biswal L, Goodwill JE, Janiak C, Chatterjee S. *Sep Purificat Rev*, In Press. <https://doi.org/10.1080/15422119.2021.1956539>.



- [61] Wang L, Zheng M, Xie Z. *J Mater Chem B*, 2018, 6, 707–17.
- [62] Chen W, Wu C. *Dalton Trans*, 2018, 47, 2114–33.
- [63] Zhu WJ, Zhao JY, Chen Q, Liu Z. *Coord Chem Rev*, 2019, 398, 113009.
- [64] Kaur N, Tiwari P, Kapoor KS, Kumar Saini A, Sharma V, Mobin SM. *Cryst Eng Comm*, 2020, 22, 7513–27.
- [65] Vassaki M, Papathanasiou KE, Hadjicharalambous C, Chandrinou D, Turhanen P, Choquesillo-Lazarte D, Demadis KD. *Chem Commun*, 2020, 56, 5166–69.
- [66] Steinert DM, Ernst SJ, Henninger SK, Janiak C. *Eur J Inorg Chem*, 2020, 4502–15.
- [67] Liu X, Wang X, Kapteijn F. *Chem Rev*, 2020, 120, 8303–77.
- [68] Rafique MM. *Appl Syst Innov*, 2020, 3, 26. <https://doi.org/10.3390/asi3020026>.
- [69] Hastürk E, Ernst SJ, Janiak C. *Curr Opin Chem Eng*, 2019, 24, 26–36.
- [70] AL-Dadah RK, Mahmoud S, Elsayed E, Youssef P, Al-Mousawi F. *Energy*, 2020, 190, 116356.
- [71] Kim SI, Yoon TU, Kim MB, Lee SJ, Hwang YK, Chang JS, Kim HJ, Lee HN, Lee UH, Bae YS. *Chem Eng J*, 2016, 286, 467–75.
- [72] Trapani F, Polyzoidis A, Loebbecke S, Piscopo CG. *Microporous Mesoporous Mater*, 2016, 230, 20–24.
- [73] Kim H, Yang S, Rao SR, Narayanan S, Kapustin EA, Furukawa H, Umans AS, Yaghi OM, Wang EN. *Science*, 2017, 356, 430–34.
- [74] Urquhart J. *Chemistry World* 2016, September 27. <https://www.chemistryworld.com/news/worlds-first-commercial-mof-keeps-fruit-fresh/1017469.article> (accessed July 27, 2021).
-  [75] Notman N. *Chemistry World* 2017, May, Vol. 14 (5), p. 44–7. <https://www.chemistryworld.com/features/mofs-find-a-use/2500508.article>
- [76] Trager R. *Chemistry World* 2016, October 28. <https://www.chemistryworld.com/news/mofs-offer-safer-toxic-gas-storage-/1017610.article?adredir=1> (accessed July 27, 2021).